Materials Transactions, Vol. 53, No. 1 (2012) pp. 234 to 239

EXPRESS REGULAR ARTICLE

Effect of Alloying Elements on High Temperature Mechanical Properties for Piston Alloy

Chang-Yeol Jeong*

Department of Nuclear and Energy System Engineering, Dongguk University, 707 Seokjang-Dong, Gyeongju 780-714, Korea

Recent legislative and environmental pressures on the automotive industry to produce light-weight fuel-efficient vehicles with lower emissions have led to a requirement for more efficient engines. Therefore, combustion pressures of diesel engines have increased up to 20 MPa and the more durable alloys for pistons are thus necessary to increase the thermal and fatigue resistance. The demand for more efficient engines is resulting in components operating under severe stress and temperature conditions. During start/stop of engine cycles, LCF (low cycle fatigue) phenomena is generated due to the thermal transient, also HCF (high cycle fatigue) and creep deformation occur under the steady-state engine temperature during operation of engine. A quantitative study of the effect of alloying elements on mechanical behavior of Al–12 mass%Si casting alloys for piston has been conducted. In the condition of minimizing casting defects, the influence of compounds features on the high temperature mechanical performance became more pronounced. Depending on Ni and Cu content affecting the strength of the matrix, the tensile strength was increased with Ni and Cu content, whereas the elongation was increased in the reverse case. Also, creep resistance was drastically increased with Ni and Cu contents mainly due to prevention of deformation owing to the increased eutectic and precipitation particles. LCF lives were decreased with alloy contents in Coffin–Manson relation because of the smaller elongation, but the analysis of fatigue lives with hysteresis loop energy which consists of both strength and elongation showed that the fatigue lives were normalized regardless of chemical compositions and test temperature. [doi:10.2320/matertrans.M2011259]

(Received August 24, 2011; Accepted October 28, 2011; Published December 14, 2011)

Keywords: *aluminum–silicon alloy, automobile, piston, fatigue, creep*

1. Introduction

There have been strong moves in recent years to produce light-weight fuel-efficient vehicles with lower emissions based upon the legislative and environmental pressures on the automotive industry. The most effective way for a light-weight car is to apply light-weight materials such as aluminium alloys. In recent years, the diesel engines are becoming prevalent because of low total emission and also combustion pressures of diesel engines have increased more and more up to 20 MPa. Thus, the microstructural parameters, i.e., the DAS (dendrite arm spacing), porosity, morphology of silicon and the second phase particles are clearly very important in the thermal fatigue and creep properties. Since many components used in automotive engines are subjected to complex loading cycles at high temperatures,[1–4] it is important to understand the loading mechanisms and damage accumulation, also to increase the fatigue and creep lives at the given situations. The aim of this study is the improvement of high temperature mechanical properties for piston materials with modifying the chemical compositions. This paper examined the mechanical properties of aluminium casting alloys made by a permanent-mold cast and evaluated the effect of alloying elements such as Cu, Mg, Ni and Fe on fatigue and creep behavior. A series of fatigue and creep tests were conducted to evaluate the deformation resistance of Al–12 mass%Si cast alloys in which chemical compositions of Cu, Ni and Fe contents are varied. Based on the experimental results, one could know that the durability of automotive parts can be increased by reinforcement of microstructure with minor change of process and alloying elements.

*Corresponding author, E-mail: jcy@dongguk.ac.kr

Table 1 Chemical compositions and the heat treatment steps of Al–Si piston alloys (mass%).

	Cu	Si	Mg	Zn	Fe	Mn	Ni	Ti	Al
Alloy A	1.00	12.14	0.78	0.049	0.61	0.012	1.20	0.02	Rem
Alloy B	2.85	11.75	1.01	0.047	0.34	0.018	2.63	0.12	Rem
Alloy C	4.89	12.21	0.76	0.033	0.20	0.110	2.83	0.13	Rem

Heat treatment
Aging: 250°C/5 h → air cooling

2. Experimental

Three types of Al–Si alloys were casted by permanent mold gravity method. The chemical composition and the heat treatment schedule of the alloys are shown in Table 1. Cylindrical type specimens for mechanical tests were machined and subsequently polished longitudinally up to 2000 grit crocus cloth to remove the machining notch effect. Strain controlled uniaxial LCF tests were conducted with the strain rate of $1 \times 10^{-3}\,s^{-1}$ at 250 and 300°C using the dynamic Instron model 8861 machines and also creep tests were carried out under the constant load control at 250 and 400°C. All the test results were recorded by using a computer data acquisition system and analyzed from the condition in which the softening and/or hardening were finished to have stable strain and stress.

3. Results and Discussion

3.1 Microstructures

Figure 1 shows the optical microstructures of cast Al–12 mass%Si matrix with different Cu, Ni, Fe and Ti contents after T5 heat treatment. The basic microstructure of the alloys

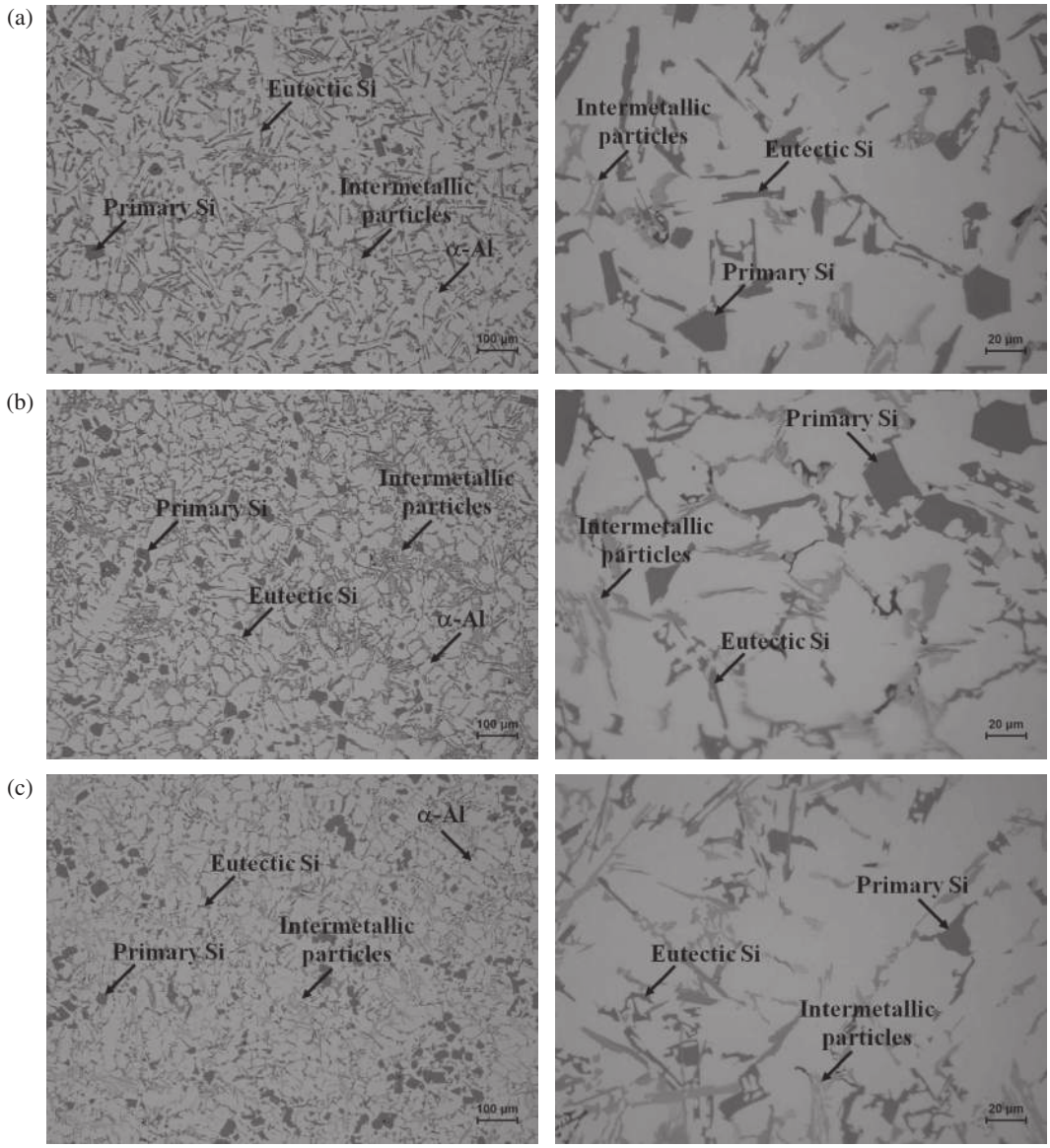

Fig. 1 Optical microscope photographs showing the microstructure after T5 heat treatment, (a) alloy A, (b) alloy B, (c) alloy C.

consists of primary Si and α-Al dendrites with eutectic Si and intermetallic particles distributed between the α and β phases to form a cell pattern periodically repeated across the metallographic surface. As can be seen in Fig. 1, the increase of Cu and Ni, the microstructure becomes finer mainly due to undercooling effect,[5–7] and the addition of Ti provides the finer α-Al formation which helps to restrict the growth of primary Si and intermetallic phases.[8] Also by the decrease of Fe content, the amount of β-Al_5FeSi intermetallics is reduced and their sizes are also decreased whereas the total amount of intermetallic particles are increased because of the increase of Cu and Ni.

3.2 Physical properties

Figure 2 illustrates the high temperature physical properties of Al–12 mass%Si casting alloy with the addition of alloying elements. Particularly Fig. 2(a) represents thermal expansion coefficient and Fig. 2(b) does elastic modulus. As the temperature is raised, the thermal expansion coefficient increases, and at the temperature of more than 350°C, it tends to be saturated. This can be explained by the fact that softening of solid with the increase of temperature more than 0.7 T_m (melting temperature) in which the general properties of solid could not be maintained. Therefore, it is thought that the reliability of thermal expansion coefficient over 350°C temperature range is limited due to the collapse of solid. On the other hand, the elastic modulus decreases almost linearly with its rise. As the increase of the portion of Cu and Ni, thermal expansion coefficient is reduced significantly at the same temperature and kept stable state in higher temperature up to 350°C whereas 300°C for the alloy A, and the elastic modulus increases as much as 5 GPa. This result is thought to be caused by Ni that is the high temperature stability content and restricts the thermal expansion and raises the stiffness and Cu that plays the role of increasing the age hardening precipitation of $CuAl_2$ and results in the increment of elastic modulus at a given temperature as shown in Fig. 2(b). Exposure to temperatures greater than 250°C for an extended period, however, will result in severe coarsening of these precipitates and causes bad effects on strengthening purposes.

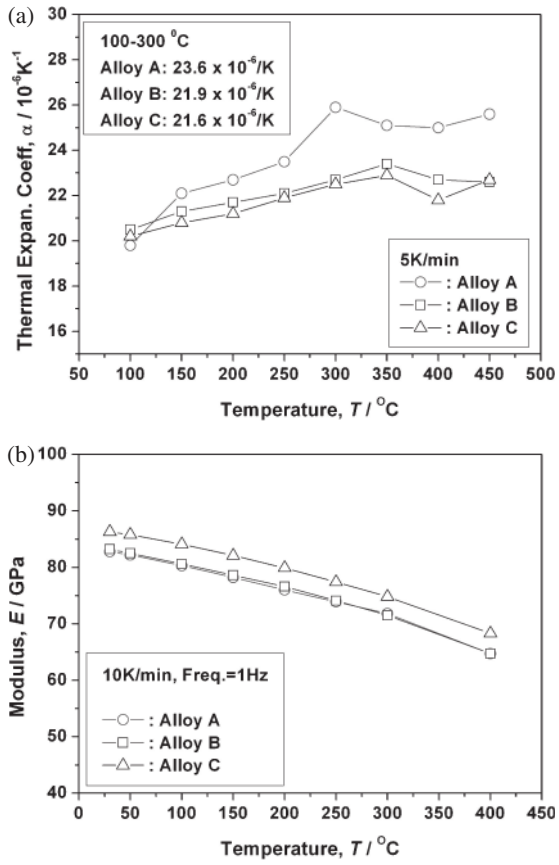

Fig. 2 High temperature physical properties for Al–12Si alloys, (a) thermal expansion coefficient, (b) elastic modulus.

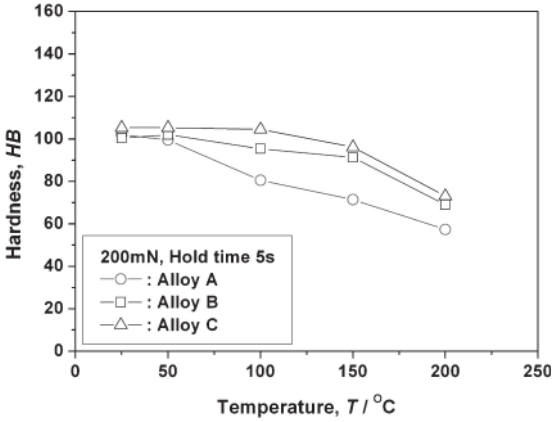

Fig. 3 High temperature hardness results for Al–12Si alloys.

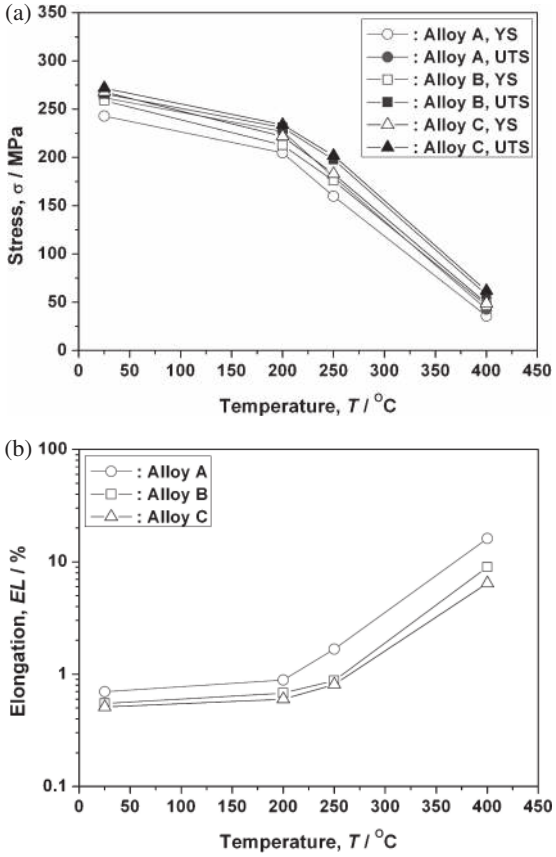

Fig. 4 Tensile test results of Al–12Si alloys, (a) YS (yield strength) and UTS (ultimate tensile strength), (b) EL (elongation).

Therefore, the enhanced Cu content requires provisions to avoid the forming of coarse $CuAl_2$ particles. It has been reported that, in this case Ni positively influences the alloy kinetics because it is almost insoluble in Al-matrix even at higher temperatures, and Ni shows the strong affinity with Cu.[8,9] The Ni containing precipitations of the type $Al_3(Ni,Cu)_2$ are stationary during aging at high temperature and can be regarded as the stabilizer for Cu, avoding the formation of coarse $CuAl_2$ particles. Increasing the Ni content also results in the formation of FeNiAl intermetallic phases which are stable at 350°C and so provide further strengthening at higher temperatures. The increase of Ni and Cu content is very effective since the key requirement of piston is keeping high temperature strength and low thermal expansion characteristics.

3.3 Mechanical properties

3.3.1 Hardness

Figure 3 shows the high temperature hardness experiment result of three alloy sets using micro indenter. As temperature is raised, hardness tends to be reduced. On the other hand, with the increase of Cu and Ni content, the hardness grows notably. For alloy A, hardness was reduced over 50°C but for alloy C, it remained over 150°C. This can be in line with the result depicted in Fig. 2 in a sense that the rise of Cu and Ni content contributes to high temperature stability.

3.3.2 Tensile property

Tensile tests were conducted to measure the mechanical properties of Al–12Si with different chemical composition and testing temperatures, and the results are shown in Fig. 4. The yield strength and ultimate tensile strength of the alloy A were 243 and 262 MPa, respectively at room temperature. However, by varying the Cu, Ni and Fe content of Al–12Si alloy, both yield and tensile strength were significantly affected. In the alloy C with increased Cu and Ni contents, yield strength was improved up to 268 MPa, and the tensile strength was 272 MPa shown in Fig. 4. Also, the tensile properties at high temperatures showed the same tendency compared with room temperature resulting in improved strength, especially yield strength. On the other hand elongation was slightly decreased as the rise of portion of

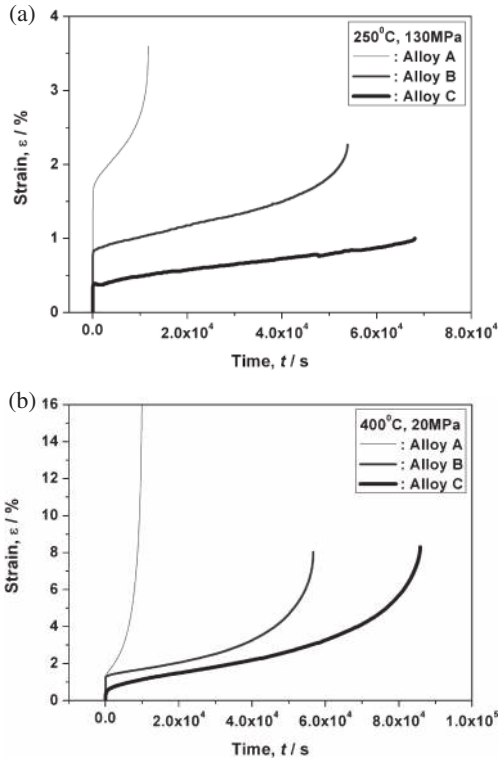

Fig. 5 Creep curves for three Al–12Si alloys, (a) 250°C, 130 MPa, (b) 400°C, 20 MPa.

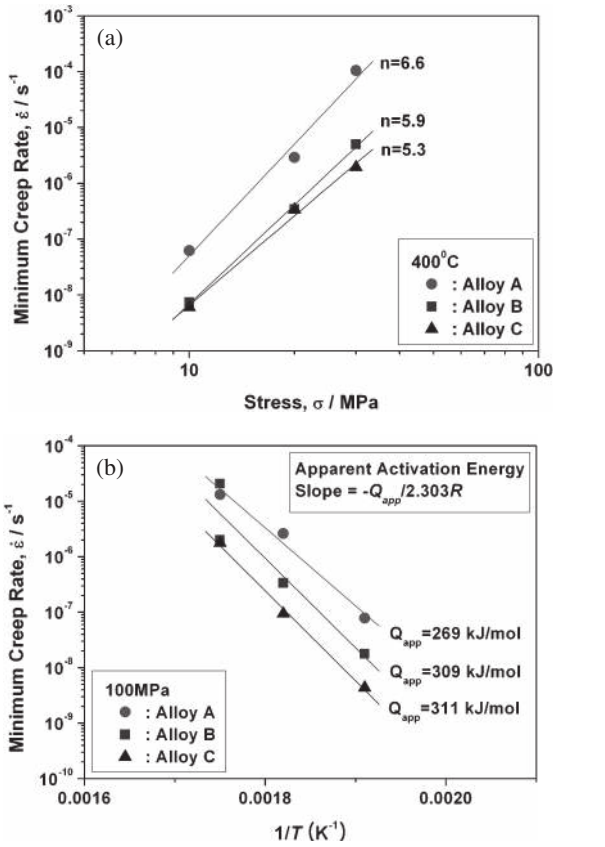

Fig. 6 Creep properties of Al–12Si alloys, (a) stress dependence creep rate, n, (b) temperature dependence creep rate, Q.

added content. This is thought to be in line with the requirement of piston alloy that is the low thermal expansion and deformation characteristics.

3.3.3 Creep property

To evaluate the high temperature deformation resistance that is the key factor of automotive piston, creep tests were conducted for three alloys and its results are summarized in Fig. 5. At 250 and 400°C, the instantanious creep strain and creep strain over time tends to decrease significantly with the increase of Cu and Ni content. It was 2.8 h for the alloy A to reach the final rupture but 23.8 h for the alloy C. This conforms the previous physical and tensile properties because of the increase of precipitation phase and high temperature stability element effect. For most of the solid materials, it has been shown that the steady state creep rate $\dot{\varepsilon}$ is related to the applied stress and temperature by,[10)]

$$\dot{\varepsilon} = A\sigma^n \exp\left(-\frac{Q_{\text{app}}}{RT}\right) \quad (1)$$

where Q_{app} is the apparent activation energy for creep, R is the gas constant (= 8.314 J/mol K), T is the absolute temperature, and A and n are the structure factor and the stress exponent, respectively. So if dislocation creep is considered, the strong dependence of creep rate on the applied stress is observed and is very important from an engineering point of view. Figure 6(a) denotes the stress dependency of creep deformation at 400°C. As the stress is increased, the minimum creep rate increases. We can also see the value of n is between 5.3 and 6.6, which is coincident with the result that the value of n for alloy should be larger considering the value of n for pure Al i.e., 5.[10)] This exponent value is the same as the values suggested from the conventional creep of several studies in the high-stress region. High values of the stress exponent are commonly obtained with precipitation and dispersion-hardened alloys,[10,11)] even though recovery processes are known to play an important role in creep of such alloys. On the other hand, the content of added element increased, the minimum creep rate was reduced significantly at the same stress and the value of n gradually decreased to 5 that is the value of pure Al. This result is thought to be caused by high homologous temperature that is above about 0.8 (400°C). Therefore, both diffusional and dislocation creep affect the value of n competitively, whereas the stress exponents are about 8–9 in 250°C, which is higher than that of 400°C because dislocation creep is more dominant in lower temperature. Figure 6(b) shows the temperature dependency of creep rate at constant stress. It has been found that the activation energy of pure Al is 150 kJ/mol which is same as the activation energy for lattice diffusion.[12)] In this study, the apparent activation energy was larger than 150 kJ/mol, and as the contents of Cu and Ni were increased, activation energy grew continuously up to 311 kJ/mol. For many of the precipitation and dispersion-strengthened alloys, it has been known that the activation energy of creep reaches values that occasionally exceed several times the values of the activation energy of lattice diffusion in the matrix.[13)] Under long-term creep conditions, particles of a proper phase, uniform in size and homogeneously distributed in the matrix, can act as effective obstacles to dislocation motion even at very high homologous temperature. However, the creep resistance need not

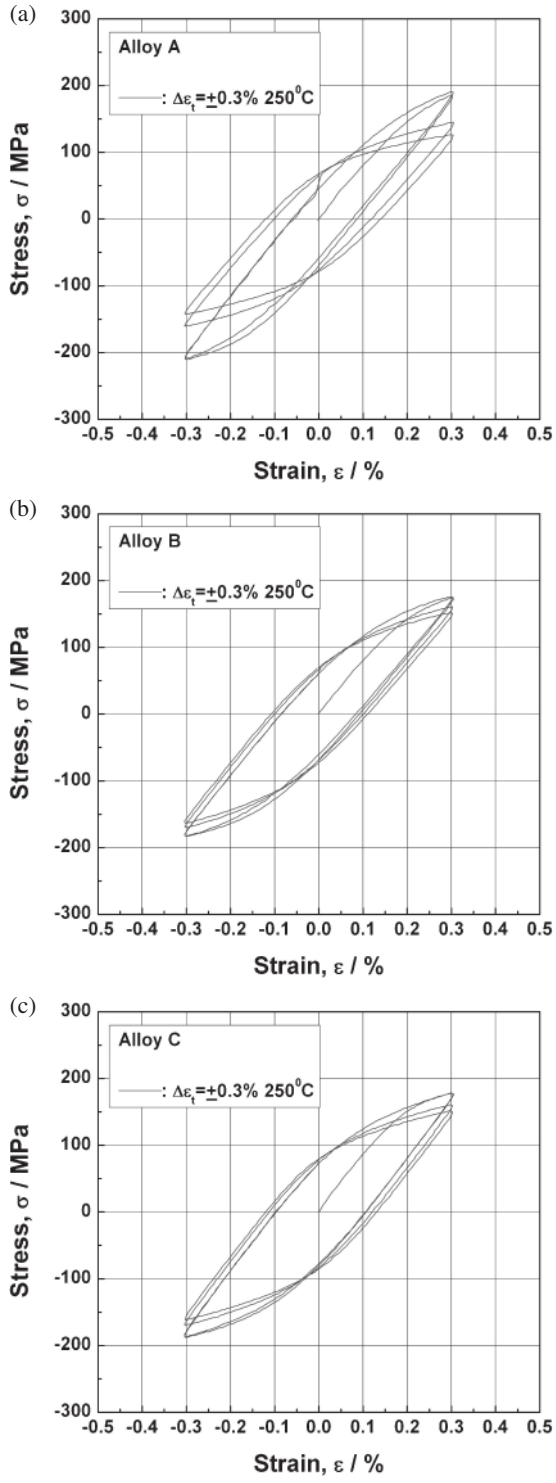

Fig. 7 Cyclic stress–strain behavior for Al–12Si alloys, (a) alloy A, (b) alloy B, (c) alloy C.

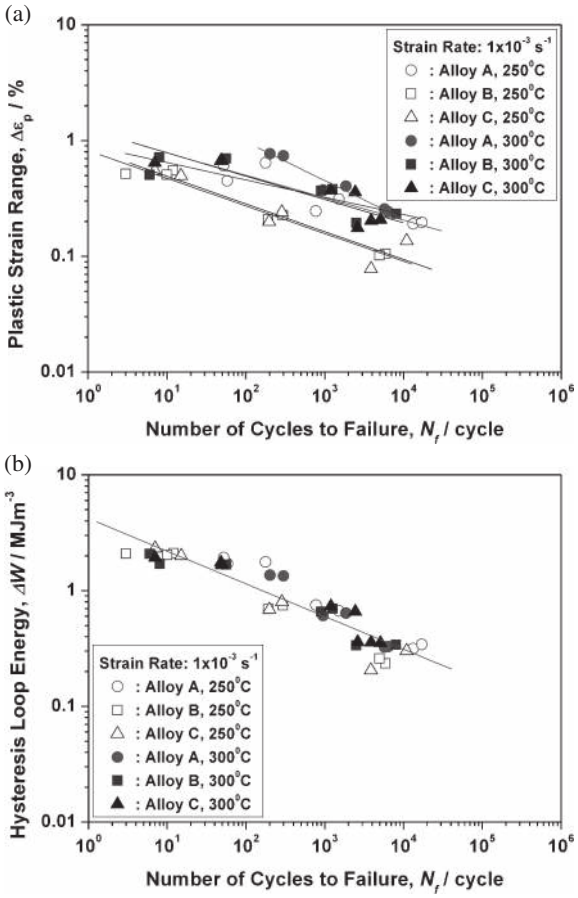

Fig. 8 Low cycle fatigue results of Al–12Si alloys, (a) Coffin–Manson relation, (b) hysteresis loop energy.

always be determined by the particles acting as obstacles to lattice dislocation glide. At high enough temperature, emission and absorption of vacancies by grain boundaries and/or grain boundary sliding and also dislocation climb by lattice diffusion can operate as the creep rate controlling process. In this case, the dominant role is played by the particles homogeneously located in the matrix, and the stable particles retard the creep deformation as well as dislocation climb and consequently result in higher activation energy than that of lattice diffusion. Since it denotes the increase of creep resistance with the addition of alloying elements, we may use this effectively for the increase of durability at high temperatures.

3.3.4 Fatigue property

Figure 7 illustrates the change of hysteresis loop according to the cyclic deformation at the condition of 250°C, $\Delta\varepsilon = \pm 0.3\%$. We analyzed the change of loop at the start and the half of fatigue life (N_f). In the case of the alloy A, we can find the obvious cyclic softening behavior that the tension and compression peak stress is gradually decreasing as the progress of cyclic deformation. For the alloys B and C, we can see that the degree of cyclic softening is greatly declining and the strength is not affected by the repeated deformation at the high temperature.

Figure 8 demonstrates the low cycle fatigue results of three alloys over multiple sets of temperature and strain ranges. When we are concerned with Coffin–Manson relation in which the fatigue life is evaluated as plastic strain range, the higher temperate and larger elongation, the longer fatigue lifes as can be seen in Fig. 8(a). If we evaluate the fatigue life only as plastic strain range, the fatigue life may be distorted as a result of considering the increase of elongation due to the rise of temperature with neglecting the strength of material. Therefore, when we evaluate the fatigue life as hysteresis loop energy that considers the strength as well as plasic strain of materials at the given condition, we can have almost

similar low cycle fatigue life without the increase of fatigue life due to the increase of temperature as shown in Fig. 8(b). Also low cycle fatigue of alloys A showed almost similar life with the increase of alloy content. Conclusively, this denotes that other high temperature mechanical characteristics can be improved without deteriorating the fatigue feature.

4. Conclusions

(1) The increase of Cu and Ni content, the finer microstructure and uniform precipitation were resulted.

(2) The thermal expansion coefficient was reduced and the elastic modulus, hardness and tensile strength were increased with Cu and Ni content at high temperature.

(3) Creep test results showed that the creep properties were significantly improved as the alloying elements were increased.

(4) High temperature fatigue results showed that the cyclic softening behavior was reduced by increasing the portion of added contents. When the low cycle fatigue lives are expressed as hysteresis loop energy that is the amount of energy consumed over a cycle, they shows the reasonable fatigue life evaluation.

Acknowledgments

This work was supported by the Dongguk University Research Fund of 2010. Thanks are given for their financial support.

REFERENCES

1) C. Y. Jeong and S. Ha: Int. J. Cast Met. Res. **21** (2008) 235–238.
2) C. Y. Jeong, C. S. Kang, J. I. Cho, I. H. Oh and Y. C. Kim: Int. J. Cast Met. Res. **21** (2008) 193–197.
3) F. Langmayr and F. Zieher: VDI-Ber **1813** (2004) 227–243.
4) J. Hadler, S. Flor and C. Heikel: VDI-Ber **1830** (2005) 285–308.
5) J. M. Boileau, J. W. Zindel and J. E. Allison: SAE 970019 (1997) 61–72.
6) K. Mizuno, E. Fan, S. Furutani, S. Yokota and T. Fukusako: J. Jpn. Inst. Light Met. **43** (1993) 618–624.
7) Q. G. Wang, D. Apelian and D. A. Lados: J. Light Met. **1** (2001) 85–97.
8) S. J. Barnes and K. Lades: SAE Technical Paper Series 2002-01-0493 (2002).
9) Mielke, Steffens, Beer and Henning: SAE Technical Paper Series 980687 (1998).
10) O. D. Sherby and P. M. Burke: Prog. Mater. Sci. **13** (1968) 323–390.
11) D. Sidey: Metall. Trans. A **2** (1976) 1785–1791.
12) O. D. Sherby and J. Weertman: Acta Metall. **27** (1979) 387–400.
13) K. Milička, J. Čadek and P. Ryš: Acta Metall. **18** (1970) 733–746.